

NaNocrystalline audio engineering materials

Eduard Fochenkov, Head of Bureau of Mechanization and Automation, Mstator JSc, Technical Consultant for Magnet Wireframe Applications, edf01@yandex.ru

The article deals with the application of nanocrystalline magnetically soft materials in audio engineering. Detailed technical characteristics are given in comparison with electrical steel and amorphous iron-based materials. Practical data and correlations obtained by experiment are given. Recommendations on application, references to information sources and calculation methods are given.

In November 2015, the Russian defense-industrial complex enterprise Mstator JSC (Borovich) celebrated its 50th anniversary. For more than 35 years the plant has been developing technologies of magnetically soft amorphous and nanocrystalline materials [1]. The field of application of these materials is quite extensive [2]. The capabilities of the materials in typical applications are described in [3-5, 18]. The author of this article is not an expert in this field and therefore can't claim how the properties of materials affect subjective perception of sound. The article attempts to reveal the physical

The properties and characteristics of materials as they apply to audio engineering.

Nanocrystalline material first appeared in Japan under the FINEMET brand in 1987. Nowadays a number of nanocrystalline materials have been developed in Germany, the United States, Israel, China, Russia and other countries. The physical properties of amorphous and nanocrystalline soft magnetic materials are explained in [1].

At present, oao mstator produces five types of nanocrystalline tapes, the properties of which are presented in Table 1.

Table 1. Properties of nanocrystalline tapes

Properties of the alloys	AMAG-200	AMAG-200S	AMAG-201	AMAG-204	AMAG-211
Saturation induction B_{10} , Tl	1,20	1,16	1,20	1,20	1,25
Coercive force N_c , A/m	0,8	0,8	1,5	2,0	3,2
Permeability μ at 10 kHz, $\times 10^3$	30 \div 80	50 \div 110	20 \div 30	10 \div 15	3 \div 8
Crystallization start temperature T_{sp} , °C	515	515	515	515	510
Curie temperature T_c , °C	570	560	>560	>560	>560
Density γ , g/cm ³	7,3	7,3	7,3	7,4	7,6
Rectangularity coefficient of the linear hysteresis loop (annealing in transverse field), not more	0,1	0,1	0,1	0,05	0,05
Specific loss P_{sp} , W/kg at frequency $F = 10$ kHz at $B_m = 0.2$ Tesla at frequency $F = 100$ kHz at $B_m = 0.2$ Tesla at frequency $F = 100$ kHz at $B_m = 0.3$ Tesla	0,5 \div 1,0 25 \div 35 55 \div 65	0,5 \div 1,0 25 \div 35 55 \div 65	1 \div 1,5 30 \div 40 -	1 \div 2 30 \div 50 -	1,5 \div 2,5 40 \div 55 90 \div 120
Saturation magnetostriction λ_s , $\times 10^{-6}$	2	0,5	3	4,5	8
Domestic and foreign alloys - analogues for use	Finemet SBDSR GMA113	Vitroperm 500F Vitroperm 800 Mastomet	Vitroperm 500F	-	Vitroperm 250F

Abbreviations used:

HG - hysteresis loop;
 AFC - amplitude-frequency response; FFC - phase-frequency response;
 K_{np} - hysteresis loop rectangularity coefficient, $K_{np} = B_r/B_m$; LF - low frequencies;
 HF - high frequencies;
 PP - Push-Pull, two-stroke tube cascade;
 SE - Single-Ended, single-circuit tube stage; LPD - nonlinear distortion coefficient;
 DAC - digital-to-analog converter;
 SRPP - Shunt regulated push-pull amplifier, a common two-amp stage; negative feedback.

properties of nanocrystalline materials can be effectively regulated by the annealing regime. Since the level of technology determines the final quality characteristics of cores, the characteristics of products from different manufacturers are far from being identical. Four types of hysteresis loops are obtained on an annealing machine, using AmAG-200 with different annealing modes: 1) rectangular (series MSSN, annealed in a longitudinal magnetic field, $K_{np} > 0.98$); 2) rounded (annealed without field, the shape reminds ferrite SG); 3) linear with maximum initial permeability (series MSFN, typical $K_{np} = 0.45$, annealed with permeability optimization); 4) maximum linear (MSTAN series, typical $K_{np} = 0.1...0.15$, optimized annealing

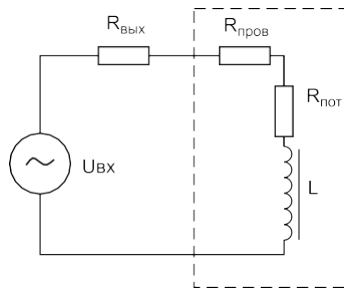


Fig. 1. Simplified equivalent series circuit of a tube cascade loaded on the transformer primary winding

by linearity). The latter series is used for audio applications.

Main features of the MSTAN series

1. saturation induction is comparable to that of iron-based amorphous alloys and transformer steel (1.16 versus 1.56 and 1.85, respectively).
2. linearity of the magnetization curve. typical rectangularity coefficient 0.1...0.15. ratio of maximum magnetic permeability to initial magnetic permeability 1.25...1.3.
3. High initial relative magnetic permeability (up to 70,000), and weak dependence of magnetic permeability on induction amplitude and frequency.
4. Low magnetic resistivity ($0.5 \cdot 10^{-6}$). About 1/40 compared to iron-based amorphous alloys, about half as low as transformer steel. less susceptible to mechanical stresses, low acoustic noise level.
5. Excellent high-frequency performance. very low losses. About 1/5 compared to iron-based amorphous alloys and about the same loss compared to cobalt-based amorphous alloys. About 1/35 compared to transformer steel (at 100 Hz).
6. excellent temperature performance and weak aging effect. amag-200c material is characterized by a change in permeability of less than $\pm 10\%$ in the temperature range $-50 \dots 150^\circ\text{C}$.
7. The toroidal shape of the magnetic cores ensures small dimensions and weight, low dissipation inductance, low active resistance of the windings and improves the quality factor of the transformer [6].

The main application of this series is in input low-signal transformers, microphone amplifiers, correctors, matching transformers after DACs,

differential stages, SRPP stages, phase-inverters, two-cycle PP cascades (interstage and output transducers), etc. without DC magnetization.

Let us consider a tube cascade loaded on the transformer primary winding. It can be represented as a voltage source with an output resistance $R_{\text{вых}}$. For simplicity we do not consider the transformer load. The theory and calculation of audio transformers are described in detail in [14, 15, 17]. The simplified equivalent series diagram shown in Fig. 1 is sufficient to understand the processes in the first approximation.

A real choke (transformer) has a winding wire resistance $R_{\text{нрроб}}$ and a magneto-wire loss resistance $R_{\text{нот}}$. As is known, the impedance vector of an inductance coil is the geometric sum of the active and reactive parts (see Fig. 2):

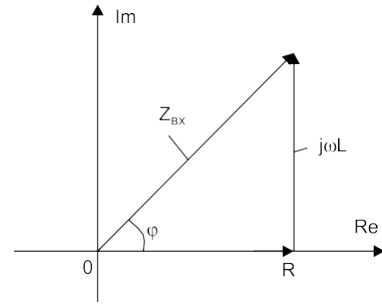


Fig. 2. Vector diagram for the inductance coil impedance

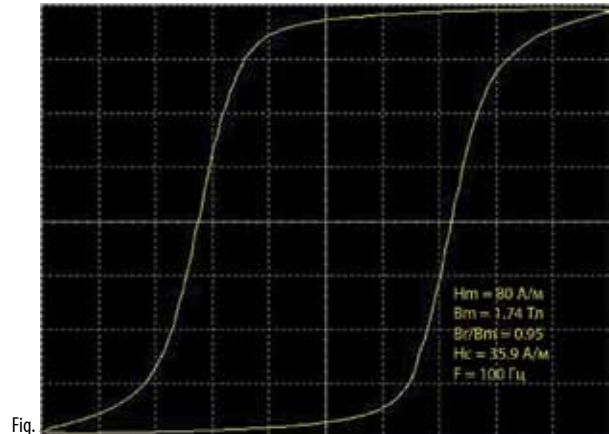


Fig.

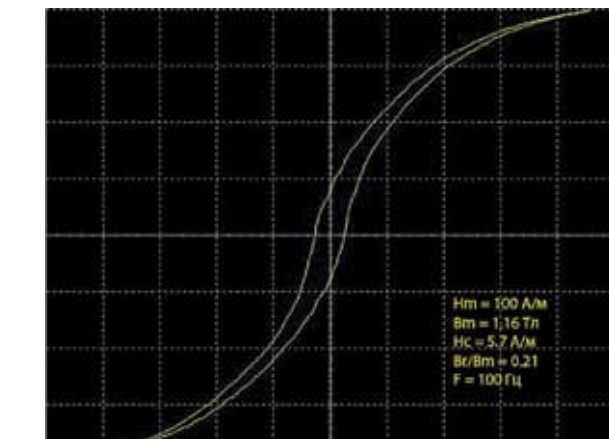


Fig.

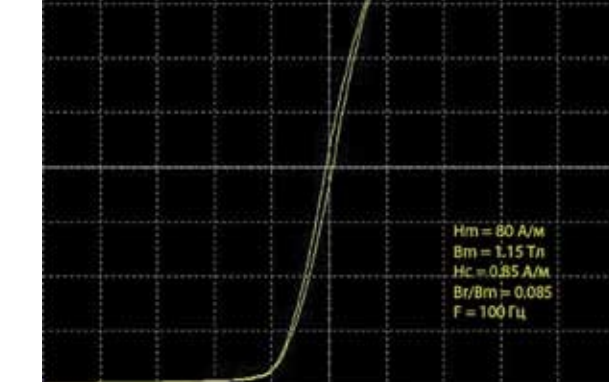


Fig. 5. Hysteresis loop of nano-crystalline alloy AMAG-200C of MSTAN series

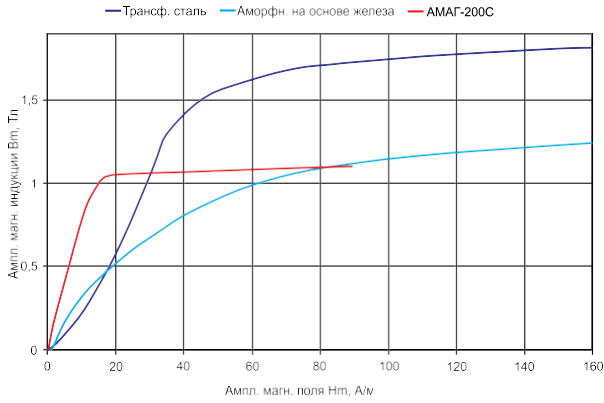


Fig. 6. Magnetization curves

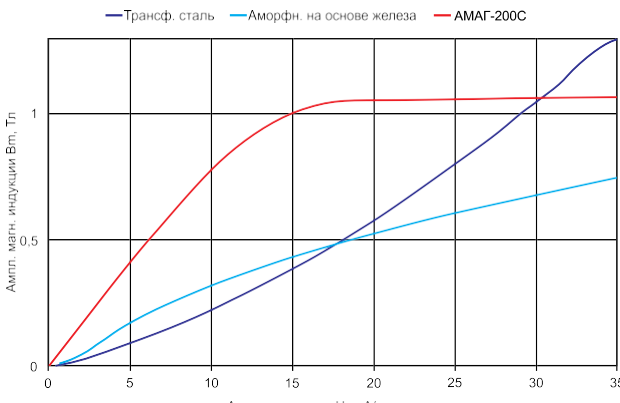


Fig. 7. Initial section of the magnetization curves

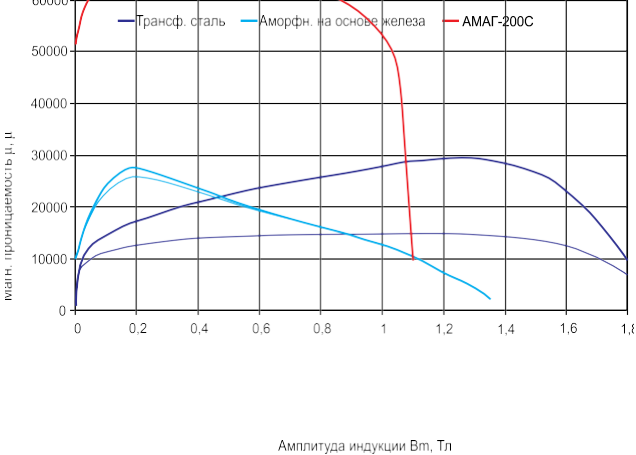


Fig. 8. Dependence of permeability on induction amplitude (F = 100 Hz)

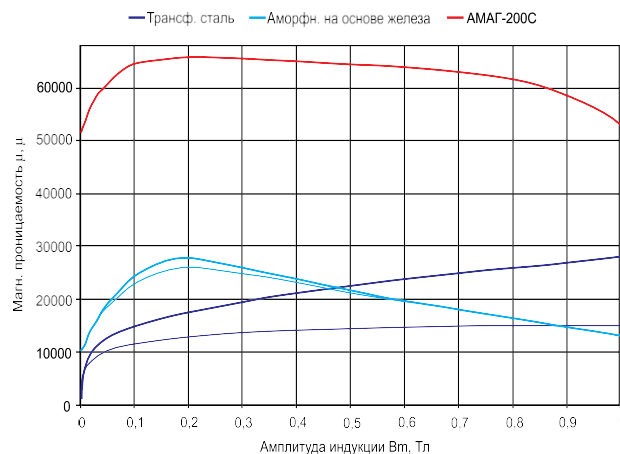


Fig. 9. Initial section of dependence of permeability on induction amplitude (F = 100 Hz)

$$Z_{ex} = R + j\omega L \quad (1)$$

In our case:

$$R = R_{prov} + R_{pot}$$

$$\varphi = \arctg(\omega L/R) \quad (2)$$

for an ideal inductance which has no losses in the core or in the wire, $R = 0$, $\varphi = 90^\circ$. The ideal inductance is linear, i.e. independent of the inductance amplitude and frequency. In this case, the ahx and Fhx of a series RL-chain (see Fig. 1) are determined by the ratio $R_{вых} / \omega L$. It is a high pass RL-filter with a boundary frequency $F_0 = R_{вых} / 2\pi L$, at which the unevenness of ahc is 3 dB and the phase shift is 45° . The important conclusion from this is that to obtain good ahc and Fx in the LF region, it is necessary either to reduce the output impedance of the tube cascade or to increase the inductance so that the boundary frequency is units of Hz.

In a real choke (transformer), losses occur in the wire and the core. real inductance is nonlinear, i.e., its value depends on the induction amplitude and frequency. But this dependence is not the same for different magnetically soft materials.

Let's compare the basic properties of three materials commonly used in audio transformers: 1) annealed cold-rolled transformer steel, strip thickness: 0.3 mm; 2) Iron-based amorphous alloy, tape thickness: 25 μm ; 3) nanocrystalline alloy amaG-200 s, tape thickness: MSTAN series. typical hysteresis loops are shown in Figures 3-5. magnetization curves are shown in Figure 6, the initial section in Figure 7. Since we are interested in the ratio $R_{вых} / \omega L$, the most practical interest is the dependence of the relative magnetic permeability on the induction amplitude and on the frequency.

Figures 8-10 show in bold lines the modulus of complex relative magnetic permeability (amplitude permeability), which is determined from the relation $\mu = B / \mu H_{m0m}$ and is given by manufacturers in specifications for different steel grades. But the inductance (and the boundary frequency) is not determined by this permeability, but by its inductive part. it is called the elastic permeability. we call it μ' . In Figures 8-10 μ' is shown with thin lines. This is because losses in the core at 100 Hz are negligible, the angle of shift between current and voltage $\varphi = 87^\circ$ (at $B_m = 1$ Tesla) and $\text{tg}\delta = R_{nom} / \omega L = 0.05$. For comparison, steel has $\varphi = 32^\circ$, $\text{tg}\delta = 1.6$ under the same conditions. **The loss resistance increases the output impedance of the tube cascade, increases the boundary frequency, worsens the AFC and FFC.** But the loss resistance for steel also depends on the induction amplitude. This means that as the signal level rises, so does the phase and ahc ! For example, Table 2-3 shows the phase and ahc of a transformer with $R_{вых} = 0.3 \omega L$ at 100 Hz, and with the same winding inductance (measured at point $B_m = 0.5$ volts). for steel the magnitude of the phase shift and the ahc drop change sharply when the inductance amplitude changes. for amaG-200 with Fx and ahc remain close to the calculated values throughout the range (for a linear RL-chain: 16,5°; -0,56 dB).

Steel is characterized by a sharp dip in permeability at low values of the induction amplitude. Magnetic domains in classical crystalline materials "stick" and a certain starting force is required to orient them. This decreases the magnetic permeability and results in "first watt effect". At low volume the sound quality

is sharply reduced. Nonlinear distortions appear, the ach and the Fx are spoiled. This effect is absent in nanocrystalline materials, where there is no usual crystalline lattice. the ultrafine crystalline structure (10-20 nm) is embedded in the amorphous matrix, the domains are very mobile and the materials work well in weak fields [1].

The nonlinearity of the magnetization curve of steel and the low permittivity in the initial region lead to three types of distortions: *nonlinear, frequency, and phase* [7]. The occurrence of nonlinear distortions due to the nonlinearity of the hysteresis loop and the influence of the material properties on the transformer quality are well described in the articles [8, 9]. It is important that the magnitude of all three types of distortion is determined by the ratio $\omega L/R_{\text{вых}}$. [The greater the ratio, the lower the nonlinear distortion coefficient, the wider the bandwidth in the LF region and the smaller the phase shift and its frequency dependence (phase distortion). Let's consider the question of distortion in a little more detail.

1. Non-linear distortion. The nonlinear magnetization curve of the magnetic material, meaning the nonlinearity of the circuit impedance, leads to current distortions. for a sinusoidal input signal this current causes a non sinusoidal voltage drop across the output resistance $R_{\text{вых}}$ of the tube stage (see Figure 1). This voltage drop is subtracted from the input sinusoidal signal. The transformer's primary winding is already receiving a difference distorted signal, which causes nonlinear distortion at the output [8]. It is obvious that as ωL grows, current and correspondingly voltage drop at output resistance $R_{\text{вых}}$ decreases, what leads to distortion reduction. To increase $\omega L/R$ ratio_{вых} as a rule, $R_{\text{вых}}$ decreases, using more powerful lamps and using feedback (the ultra-linear stage). But it is obvious that the $\omega L/R$ can be increased_{вых} and the nonlinear distortion reduced by using high permeability materials (inductance is increased) and a linear hysteresis loop (the very cause of the nonlinear distortion disappears).

2. Frequency distortion. At $F_0 = R_{\text{вых}}/2\pi L$ there is a 3 dB drop in the LF region (for an unloaded trans-former). Using nanocrystalline materials, it is easy to obtain an inductance of 500-700 Gn with a small number of turns. In this case F_0 is usually a few Hz and the primary impedance has little or no effect on the input impedance of the transformer.

induction and frequency. In this case, even at the same (in comparison to

The bandwidth of a nanocrystalline material is significantly wider in both directions due to the small losses (e.g., in an SE using a gap) than in steel. In the HF region, the scattering inductance and the reduced capacitance of the transformer are decisive. High permeability significantly reduces the magnetic flux leakage, ensures good electro-magnetic coupling and reduces the value of leakage inductance. Fewer turns are required for good ach at HF, which consequently reduces the reduced capacitance of the transformer. The resonant frequency of toroidal transformers with nanocrystalline alloy is much higher than that of classical transformers. According to [6], the toroidal core shape is optimal. For example, the typical value of leakage inductance for output toroidal transformers with a high magnetic permeability alloy is 1.3 mGn.

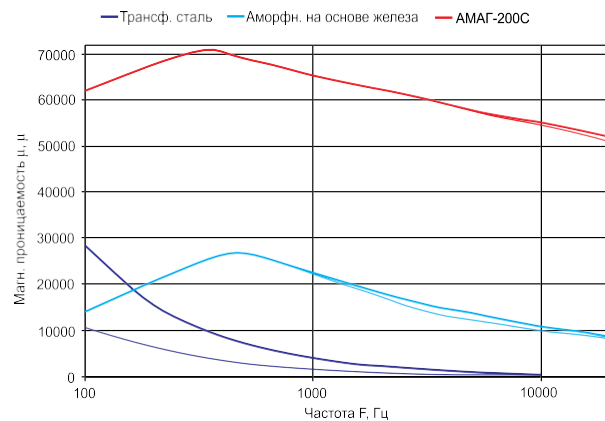


Fig. 10. Dependence of permeability on frequency at constant input voltage ($B_m = 1$ Tesla at $F = 100$ Hz)

Table 2. Frequency response, ° ($F = 100$ Hz)

B_m, Tl	0,01	0,05	0,1	0,5	1	1,5
Transformer steel	32	14,6	10,6	4,7	2,6	1,8
AMAG-200S	17,5	16,6	15,9	15,8	16,7	-

Table 3. AFC, dB ($F = 100$ Hz)

B_m, Tl	0,005	0,01	0,02	0,1	0,5
Transformer steel	-3,8	-2,8	-2,1	-1,8	-1,0
AMAG-200S	-0,55	-0,51	-0,54	-0,57	-0,5

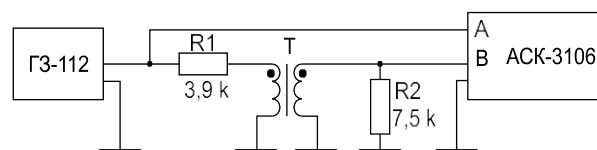


Fig. 11. Measurement scheme

of EI transformers, this value is 19 mGn [6]. For nanocrystalline alloys, due to the low scattering inductance and small parasitic capacitances, the frequency range extends to frequencies of the order of 200 kHz and higher. These frequencies are not audible, but the wide range is important for reducing phase distortions and enabling oscillations [6].

3. Phase distortion is difficult to see with a sine wave generator and oscilloscope, but for a complex signal, such as a rectangular signal that is a series of harmonics, each harmonic is shifted at different angles, and as a result, the output signal takes

a very different form. For more details about phase distortions see [7]. [7]. As ωL increases, the phase shift decreases. At frequency $F_0 = R_{\text{вых}}/2\pi L$ the angle of phase shift for unloaded trans-former is 45° (for the loaded - less). Increasing inductance up to hundreds Gn we lead frequency F_0 into region of infrasound. For such transformer the phase shift in audio range 20 Hz...20 kHz approaches to zero and it does not depend on frequency much [6]. thus, the phase shift in audible region is absent.

Note that for a signal with a stable amplitude, the induction amplitude decreases in inverse proportion to the frequency ($B_m = 1 \text{ tl at } F = 100 \text{ Hz; } B_m = 0.01 \text{ tl at } F = 10 \text{ kHz}$), and this in turn further reduces the permeability of the steel (see Fig. 9). At high frequencies, the core always operates in the initial section of the GHG, where the steel permeability is already around 1000 at 100 Hz, and is further reduced due to HF losses. Figure 10 shows the actual frequency dependence of the elastic permeability μ' at stable

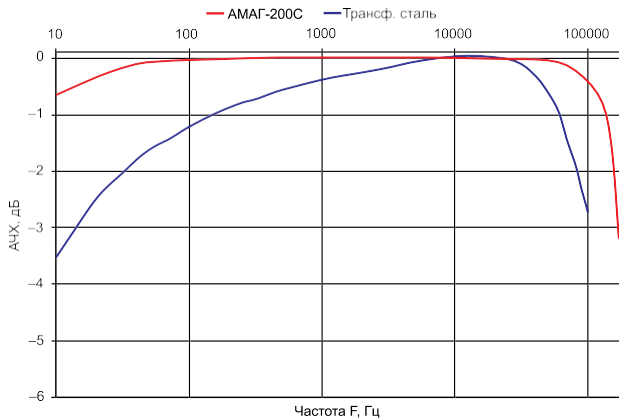


Fig. 12. AFC of transformers

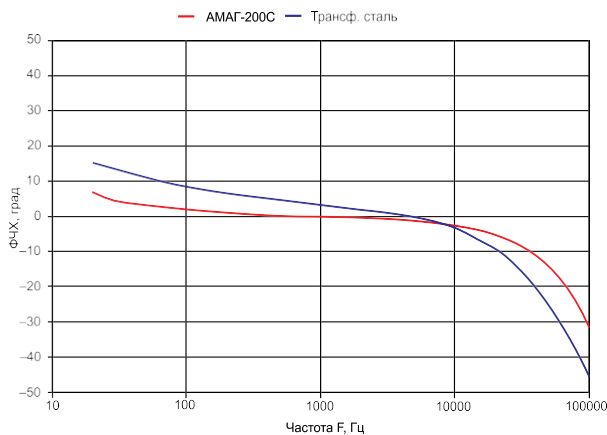


Fig. 13. FFC of transformers

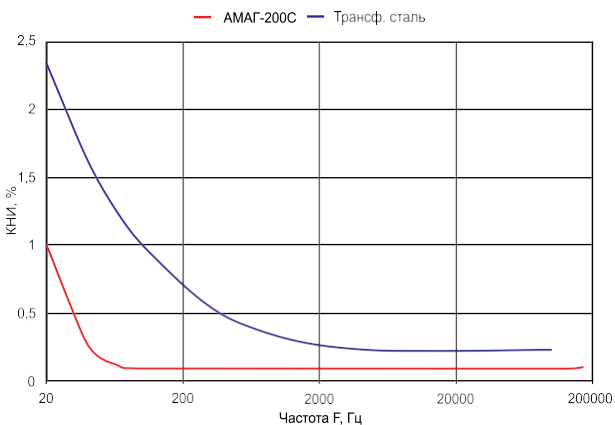


Fig. 14. The DER of transformers

Because of the decreasing induction amplitude (see Fig. 10) the permeability for amag-200s and Fe-based amorphous alloy first increases with increasing frequency and then decreases. For steel at 100 Hz $\mu' = 10600$, at 1 kHz $\mu' = 1500$, and at 10 kHz $\mu' = 220$! The low permeability of steel at HF degrades the electromagnetic coupling, increases the inductance of the scattering, and spoils the Fx. In the HF region the steel core is practically dead, the signal transmission is mainly through the interwinding capacitance. For these reasons the bifilar winding is often used in interstage transformers to obtain a good HF achromatic response. Due to the high distributed capacitance of the long coupled line the transformers have a good ach in the HF region. Some audio enthusiasts like the sound of bifilar transformers, some do not. It is difficult to judge who is right, but bifilar winding is not necessary in low loss and high permeability materials.

Another classic way to ensure good properties is to sectionalize by winding thickness to improve electromagnetic coupling and reduce capacitance. The design of such transformers is far from simple. The characteristics greatly depend on winding methods, winding direction, insulation material, number of sections and how they are connected [14-17]. In inverting and non-inverting transformers the characteristics can be very different. For example, a well-known manufacturer, Hashimoto, says: "winding methods are the result of a lot of trial and error. The ultimate goal is to find the best layout that minimizes leakage inductance and stray capacitance. The design contains an optimally chosen number of vertical and horizontal sections with an optimal method of interleaving". The initial permeability for the MSTAN series at 100 kHz exceeds 30000. In this case, a good interstage transformer can be obtained on a torus, using sectioning by sectors around the circumference, rather than by layers across the thickness of the winding. For example, a torus is divided into six 60° sections. The primary and secondary winding sections are alternated: three sections of primary winding and three of secondary winding. The distributed capacitances of the windings are reduced by the series connection of the sections. Since the capacitive coupling of the windings in this case is mainly through the core, the interwinding capacitance is also small due to the thickness of the magnetic core container material. For example, for an intercascade transformer on a torus of 60-40-30 mm (D-d-h) with two windings of 1000 turns each, the interwinding capacitance is about 75 pF, which is an order of magnitude smaller than the capacitance of designs with winding thickness sectioning and two orders of magnitude smaller than the capacitance of bifilar designs. Due to the toroidal shape of the core, high permeability and alternation of the sections, the leakage inductance is in the order of units of mGn. Such a transformer works at HF due to the properties of the magnetic material of the core and not due to the capacitive and air electromagnetic coupling of the windings.

As an illustration, consider an interstage transformer. Output resistance of the stage: 3.9 kohm; given input resistance of the transformer: 15 kohm; load resistance: 7.5 kohm ($K_{mp} = 1.43$); maximum input voltage: 30 V at 50 Hz. Let's take two magnetic cores of size 45-25-20 (D-d-h) made of amag-200s and annealed transformer steel (0.3 mm). Assuming $B_m = 1.0$ Tl at 50 Hz at $U_{ex} = 30$ V, the number of winding turns $W1 = 1000$, $W2 = 700$. The wire has a diameter of 0.2 mm. Recall that the amag-200s transformer is circularly sectioned (six alternating 60° sectors), which is not practical for steel due to its low HF permeability. In a steel transformer, the primary winding is divided into two sections. The winding sequence is: half of the primary winding across the current - secondary - second half of the primary. For amag-200s the primary inductance $L = 110$ Gn, leakage inductance $L_{pacc} = 9$ mGn, interwinding capacitance $C_{1-2} = 190$ pF. For steel, respectively: $L = 19$ Gn; $L_{pacc} = 1.3$ mGn; $C_{1-2} = 2500$ pF. Due to the absence of winding overlap [14], the inductance of the AmAG-200s scattering is higher, but the interwinding capacitance is 13 times lower.

Figure 12 shows the ach of the transformers, Figure 13 - Fhc, Figure 14 - kNi. Figures 15-16 show the meander shape at the transformers output. Note, for steel, the achx and the Fx at low frequencies are significantly lower, and we did not use the entire induction reserve of steel, taking only the

It is obvious that in order to improve the HF characteristics of steel, either the size of the transformer must be increased or the number of turns must be increased. thus, high steel induction for PP does not give a gain in the size and weight of the transformer.

material conclusions for PP and other DC bias-free stages

1. Transformer steel

for the push-pull cascade, the steel-based transformer gives the worst result and requires obligatory corrective measures (feedback). As measures to improve the situation in PP you can:

- choose the steel grade with maximum PG linearity, maximum initial permeability and minimum losses;
- use a minimum tape thickness of 0.08 mm or less;
- use a small gap to improve linearity;
- eliminate the use of a non-cut torus (any cut gives an effective gap);
- to use the shift of the operating point of the GCB from zero to the most linear section (due to the asymmetry of the DC arms);
- increase the weight and dimensions to reduce the induction range;
- to minimize the output resistance of the tube stage;
- to use a composite magnetic core made of two materials.

The latter method was described in [10]. In terms of its magnetic properties, a composite core consisting of two cores with the same center line and cross-sectional area S_1, S_2 is equivalent to a core with cross-sectional area $S = S_1 + S_2$ of a magnetic material having the following characteristics:

$$B = \eta_1 B_{11} + \eta_2 B_{22}, \quad (3)$$

where $\eta_1 = S_1/(S_1+S_2)$; $\eta_2 = S_2/(S_1+S_2)$.

the magnetic permeability of such a core:

$$\mu = \eta_1 \mu_1 + \eta_2 \mu_2. \quad (4)$$

suppose the composite core is 80% transformer steel with initial permeability $\mu_{H01} = 1000$ and saturation induction $B_{S1} = 1.9$ Tl, and 20% amag-200 s, which has $\mu_{H02} = 90000$ and $B_{S2} = 1.2$ Tl. then

characteristics of the composite core $\mu_{H0} = 18800$, $B_s = 1.76$. This method improves the dependence of permeability on induction, eliminates the "first watt effect" and reduces distortion at a reasonable cost. At low induction amplitude (high frequencies or weak signal) nanocrystalline material works, at high (low frequencies with high power) - steel. the core has both high initial permeability and sufficiently high induction, which reduces the required size and price.

2. Amorphous iron-based alloys

In PP they give good results due to small tape thickness, small losses, high initial permeability, high saturation induction. good price/quality ratio. It is desirable to take measures to reduce the output resistance of the tube cascade, to choose magnetic circuits with maximum linearity (optimal annealing), to use oos.

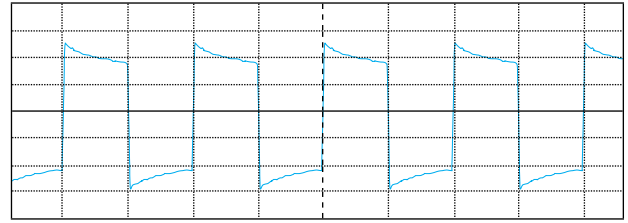


Fig. 15. Meander waveform from the output of a steel-based transformer (F = 1 kHz)

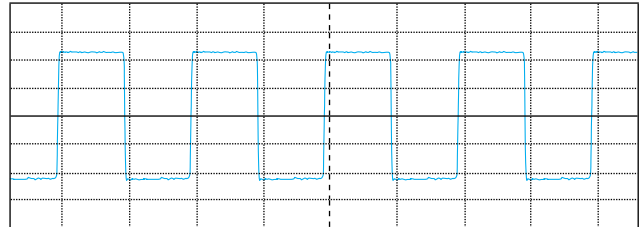


Fig. 16. Meander waveform from the AMAG-200C transformer output (F = 1 kHz)

3. AMAG-200 C

Nanocrystalline materials with high permeability give the best results in PP, low nonlinear, frequency and phase distortion even without taking measures to reduce the output resistance and without using feedback. they provide minimal size and weight of the toroidal transformer, excellent quality factor, good EMC and low leakage inductance, wide frequency range, low noise, high kPd. the toroidal core shape is optimal [6, 11]. However, these materials require that special stringent measures be taken to symmetrize the DC shoulders. This is very important, otherwise good characteristics cannot be obtained. Often a constant current of 1-2 ma will cause the magnetic core to saturate. In interstage transformers this is 5-10% of the quiescent current of the tube. For good functioning of the output transformer it is necessary to ensure that the quiescent current imbalance of the tubes is not more than 0.5% [6]. For this purpose current sources in the anodes of the tubes or special bias modules are used [6, 13].

It is not always advisable to provide the highest permeability. oo mstator produces a range of five nano-crystalline materials with an induction of about 1.2 Tl and different permeability (see Table 1). Using a material with a lower permeability, for example, a reasonable compromise can be made on the quiescent current imbalance of the tubes, or a small DC bias current in the SE interstage transformers can be achieved.

Single-cycle SE cascades

In this case a requirement unacceptable for high permeability materials appears - operation with displacement, which excludes the use of an open-circuit current. however, there is a way to use all the described advantages of the material by complicating the circuit. This configuration is mentioned in [12]. The compensation winding can have fewer windings and a correspondingly higher current. It is necessary that the bias source has a high resistance and a small capacitance, otherwise it will be a tangible additional load for the tube stage.

However, classically in SE, split magnetic conductors with a gap are used. The gap does a very useful thing - it linearizes the SG and reduces the loss angle tangent (the SG becomes narrower). As a result, the magnetic permeability weakly depends on the induction amplitude and on the frequency. As a consequence the nonlinear, frequency and phase

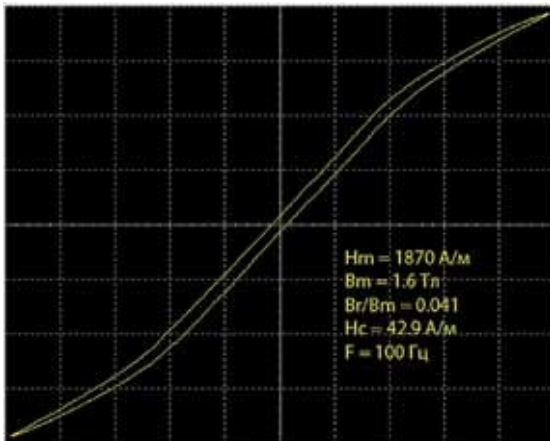


Fig. 17. Hysteresis loop of transformer steel with gap

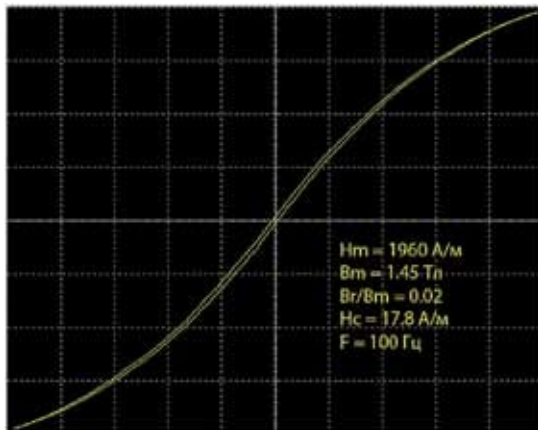


Fig. 18

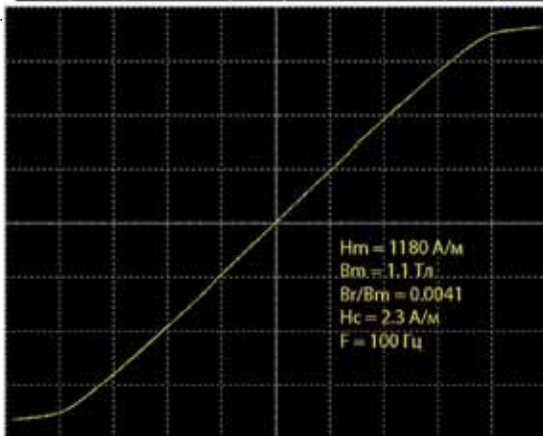


Fig. 19. Hysteresis loop of AMAG-200S with gap

distortion. the operating bias current in the SE takes the operating point from the problematic zero to a very linear section.

Unfortunately, the non-magnetic gap destroys the main advantage of amorphous and nanocrystalline alloys - the high permeability. it becomes exactly the same as in steel, and even lower, because the induction margin is smaller. The high induction gives steel the unquestionable advantage of being able to work with the highest displacement and the smallest transformer dimensions. with the appearance of the gap new materials do not have the advantage of good coupling, the dispersion inductance increases. special winding techniques, optimal sectioning, etc. are required, just as with steel. But then does it make sense to use new materials in SE? It turns out it does. Figure 17 shows the SG of transformer steel with a gap, Figure 18 shows the SG of amorphous alloy

based on F_e , Figure 19 is the PG for the alloy amaG-200 s. The gap is chosen so that the permeability was comparable - about 850. operating frequency: 100 Hz. The loops are different both in width (losses) and linearity. the point is that the initial PG affects the resulting PG. Recall the formula for torus permeability with gap:

$$\mu = \frac{l}{1 + \frac{l}{\delta \mu_0}}, \quad (5)$$

where l is the length of the midline; δ is the gap; μ_0 is the initial magnetic permeability.

In the denominator there is a numerator which is inversely proportional to the initial permeability before the cut. It can be seen that for AmaG-200 the loop is very linear and has no hysteresis visible to the eye! So the high permeability of the material does work, but in a different quality. In push-pull stages without bias we significantly reduced the nonlinear, frequency and phase distortion due to the high inductance and the very small voltage drop through the output impedance of the tube stage. In the SE stages, we again get better results in quality, but at the expense of excellent loop linearity and negligible loss tangent. Figure 20 shows the dependence of the modulus of complex relative magnetic permeability on the induction amplitude. Figure 21 shows the dependence of permeability on frequency. For amag-200s these dependences are very small, i.e. it's almost a perfect linear inductance! as a consequence, there is no distortion in the principle of all three above mentioned types. for steel with a gap at 100 Hz the permeability depends much less on the inductance amplitude than for steel without a gap (see figure 8). The ratio of the maximum permeability to the initial permeability is about 1.5, $\text{tg} \delta \approx 0.07$, and this is already good. However, there is a significant dependence of $\text{tg} \delta$ and, consequently, of the phase angle ϕ between the coercive voltage and the frequency F (see Fig. 22). The gap reduced phase distortion, but did not eliminate it completely. It is possible, therefore, that some audiophiles prefer pentodes with high output impedance, which reduce these phase distortions and partially compensate the ugly dependence of the speakers impedance on frequency (current source mode), since the amperage depends on current, and not on voltage.

conclusions on single-cycle cascades

1. **Transformer steel.** The following is a good example of how to reduce phase distortion, to use the most linear section of the core, to choose steel with the smallest possible band thickness and maximum linearity of the core.
2. **Amorphous materials based on Fe.** Due to induction comparable to steel, high initial permeability and low losses it is a good option for output transformers. best price/quality ratio, low distortion.
3. **Nanocrystalline materials with high initial permeability and clearance.**

Advantages: Excellent performance due to perfectly linear PG and negligible losses. minimal distortion. inductance is linear.

Disadvantages: larger size and weight compared to steel and amorphous materials due to lower induction. High price. Like comparable materials, they require very high quality winding with all measures to reduce parasitic capacitances and inductance of dissipation.

And finally, information to ponder on the alternative of the gap. traditionally, it was thought that any ferromag-

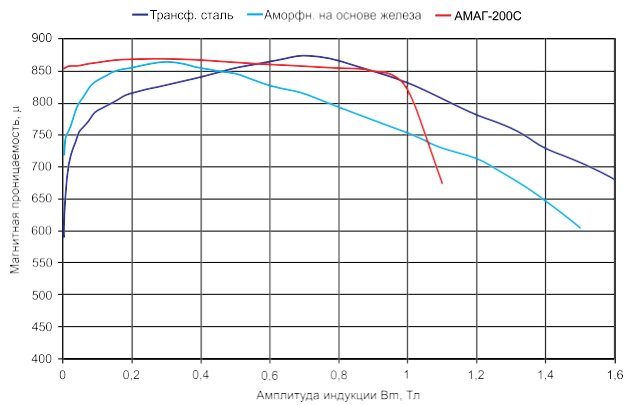


Fig. 20. Dependence of permeability on induction amplitude for cores with a gap

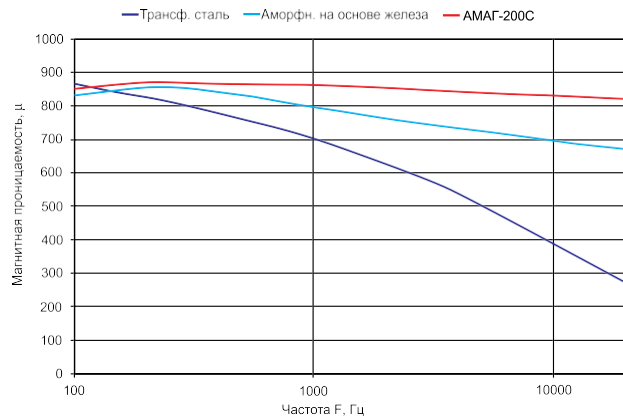


Fig. 21. Dependence of permeability on frequency for cores with a gap

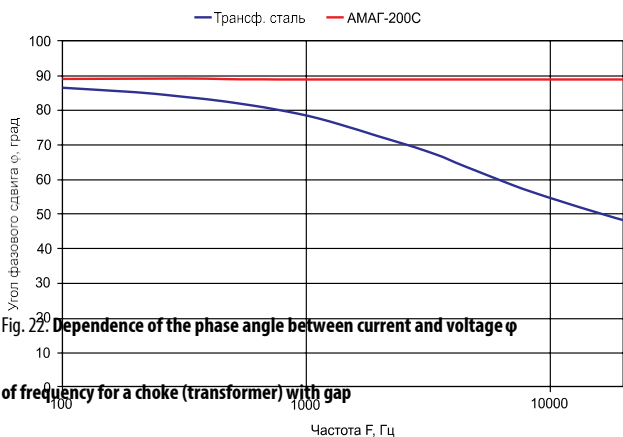


Fig. 22. Dependence of the phase angle between current and voltage φ of frequency for a choke (transformer) with gap

However, due to the further development of technologies the mass production of modern materials with linear hysteresis loop and small enough permeability has been mastered. The small permeability and linearity are provided not by the gap, but by the composition and thermomagnetic treatment. For example, amorphous iron-nickel alloy amag-223 has a permeability of 1800, saturation induction - 1.35, small losses and linear hysteresis loop (see Fig. 23). For amag-223, if the induction amplitude changes in the range of 0.05-1.1 T, the magnetic permeability μ changes in the range 1920...1800.

More expensive amorphous alloys based on cobalt amAG-186 c, amAG-186 B, amAG-186 a have saturation induction, respectively, 1.0; 0.9; 0.85 T and permeability, 1400; 2200; 3300, respectively. These materials are successfully used in precision current sensors, have a linear

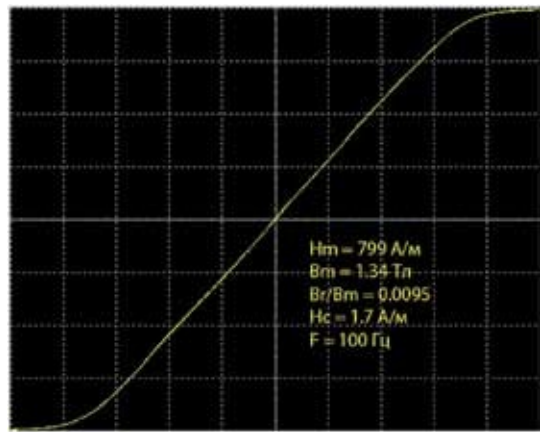


Figure 23: Hysteresis loop of iron-nickel alloy AMAG-223

The PGs, similar in shape to the amaG-223 (see Fig. 23), and can also be used in SE stages with DC bias, for example in inter-stage transformers.

In the near future a simplified calculator (in Microsoft Excel) for approximate calculation of toroidal audio transformers is planned to be posted on the mstator website in the "design center" group.

Literature

1. Amorphous and nanocrystalline magnetically soft alloys//www.mstator.ru.
2. Tapes of amorphous and nanocrystalline alloys AMAG//www.mstator.ru.
3. Э. Фоченков. Programs for calculation of winding products in pulse converters. *Electronic Components*. № 2. 2014.
4. Э. Фоченков. Application of saturable amorphous magnetic cores of MSSA series in multichannel pulse power supplies//www.mstator.ru.
5. Э. Фоченков. Application of small-sized interference-suppressing magnetic cores made of amorphous metal alloys". *Radio*. № 2. 2003.
6. Ir. Menno Van der Veen. Wide bandwidth toroidal audio signal transformers. *Lecture by the designer*//www.trafco.rs/tubeaudio-ru.php.
7. E. Snigirev. Frequency, nonlinear and phase distortions//www.musicangel.ru
8. James Moir. GA3. 1994. Output transformers//www.musicangel.ru.
9. Transformers in Push-Pull Amplifiers. Dr. Tom Hodson. *Single-ended Amplifiers, Feedback and Horn: Some History*. Sound Practices. Spring. 1994//www.musicangel.ru.
10. M. A. Rosenblat. *Magnetic Elements of Automatics and Computational Technology*. Moscow, "Nauka". 1966.
11. Ir. Menno Van der Veen. Modern High End Valve Amplifier based on toroidal output transformers//www.mennovanderveen.nl.
12. Ir. Menno Van der Veen. Universal system and output transformer for valve amplifiers. 118th AES Convention 2005. Barcelona. Paper 6347//www.mennovanderveen.nl.
13. Ir. Menno Van der Veen. Why auto-bias sounds so good//www.mennovanderveen.nl.
14. N. Starodubtsev. *Theory and Calculation of Low Power Transformers*. IP RadioSoft. 2005.
15. Y. S. Rusin. *Transformers of Sound and Ultrasonic Frequency*. L. Energy. 1973.
16. Y. S. Rusin. Determination of the intrinsic capacitance of windings. *Radiotekhnika*. № 2. 1964.
17. I. C. Tsykin. *Low frequency transformers. Theory, calculation and design*. M. Svyazizdat. 1955.
18. B. S. Chernov, O. G. Ivanov et al. *Russian Amorphous and Nanocrystalline Magnetic Materials: Physical Properties and Application*. M. Science-Intensive Technologies. № 10. 2008.